Effect of Exceptional Valine Replacement for Highly Conserved Alanine-55 on the Catalytic Site Structure of Chymotrypsin-Like Serine Protease

Mayuko TAKEDA-SHITAKA* and Hideaki UMEYAMA

School of Pharmaceutical Sciences, Kitasato University, 5–9–1 Shirokane, Minato-ku, Tokyo 108–8641, Japan.
Received March 9, 1998; accepted June 6, 1998

The catalytic triad consisting of His57, Asp102 and Ser195, which is completely conserved within the chymotrypsin-like serine protease family, plays a central role in catalysis. Highly conserved Ala55 also likely plays an important role in catalysis due to its location just behind the catalytic triad. The only exception to the conserved Ala55 in mammalian serine proteases is Val55 in bovine protein C. Interestingly, it has been demonstrated that the replacement of Ala55 with Thr results in the reduced activity of plasmin in patients with venous thrombosis and with retinochoroidal vascular disorders, which indicates the importance of Ala55 in catalysis. In the present study, we constructed a bovine protein C model which shows that Val55 causes no serious rearrangement of the catalytic site structure. We also constructed an A55T variant model of trypsin for comparison. The A55T substitution alters His57 into an inactive conformation, forming an unusual hydrogen bond between Thr55 Oγ1 and His57 Nε2. The present study shows that the Ala/Val55 residue contributes heavily to the active conformation of His57 and enables His57 to accept a proton from Ser195 Oγ effectively.

Key words serine protease; bovine protein C; homology modeling; molecular dynamics simulation

In the chymotrypsin-like serine protease family, the completely conserved catalytic triad consisting of His57, Asp102 and Ser195 (Fig. 1, chymotrypsinogen numbering is used in the present paper) plays a central role in catalysis. The catalytic roles of these residues have been well established by experimental[1—4] and theoretical[5,6] evidence. Serine proteases catalyze the hydrolysis of amides and esters by nucleophilic attacks on the carbonyl carbon of the scissile bond by the hydroxyl group of Ser195. His57 acts as a catalytic base which enhances the nucleophilicity of Ser195 and assists proton transfer from the serine hydroxyl to the substrate leaving group. Asp102 Oδ atoms (Oδ1 and Oδ2) stabilize the side-chain conformation of His57 that is required for catalysis by accepting hydrogen bonds from His57 Nδ1.

Neighboring residues of the catalytic triad, such as Cys42, Gly43, Ala55, Cys58, Tyr/Phe/Trp94, Gly196, Gly197 and Ser214, are also highly conserved in both the primary and tertiary structures.[7,8] These residues, together with the catalytic triad, stabilize one another by intramolecular interactions conserved in serine proteases, which maintain the active conformation of the catalytic triad (Fig. 1). Among the conserved neighboring residues, Ala55 seems to be very important for catalysis, because X-ray structures show that Ala55 Cβ is located just behind the catalytic His57 and Asp102. Position 55 seems to always be a small Ala because of its steric requirement. In sequenced mammalian serine proteases, the serine protease domain of bovine protein C (BOPC) is the only exception in which the conserved Ala55 is replaced with Val.[9] In other serine proteases which are highly homologous to mammalian ones, Val55 is found only in plaice trypsin.[10] As for plaice trypsin, looking at the primary structures, Rypniewski *et al.*[11] showed that it seems to be difficult to accommodate a larger side chain without disrupting the alignment of the catalytic residues or causing a major rearrangement of the neighboring structure. No theoretical studies have ever been undertaken to investigate the effect of Val55 upon the structure of the catalytic site by X-ray analysis or modeling study.

Interestingly, it has been demonstrated that the reduced activity of human plasmin in patients with venous thrombosis and with retinochoroidal vascular disorders results from replacing Ala55 with Thr in the serine protease domain.[12—17] These show the importance of Ala55 in serine protease catalysis. Previous experimental studies of A55T plasmin demonstrated that the patients possess normal levels of plasminogen antigen, and that its Michaelis constant is very similar to normal ones. In spite of these normal properties, A55T plasmin has low activity on the synthetic substrates.[18,19] These experimental results indicate that the cause of the reduced activity of A55T plasmin is localized in the catalytic site, whereas the overall structure of A55T plasmin is normal. Surprisingly, although Val and Thr are not very different from each other in size, BOPC is active, while A55T plasmin is not. It has been considered that Ala is preferable at position 55 simply because of its small size, but these examples indicate that the

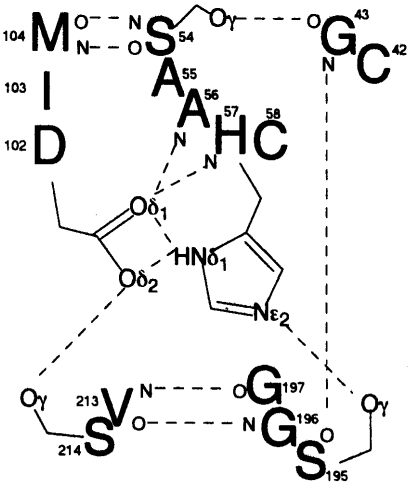

Fig. 1. Schematic Representation of the Hydrogen Bonding Network in the Catalytic Site of Bovine Trypsin

In bovine protein C, positions 54, 55 and 104 are Thr, Val and Ala, respectively. In order to act as the catalytic base, His57 must conform to the following conditions: i) monoprotonated His57 at optimum pH must be protonated at Nδ1, not Nε2, and ii) His57 must be stabilized in the conformation in which Nε2 can accept a proton from Ser195 Oγ.

* To whom correspondence should be addressed.

role of the residue at position 55 is more important and complex than earlier supposed.

In the present paper, we investigated the structural features of the catalytic site of BOPC, and compared them with serine proteases containing Ala at position 55 (Ala55 serine proteases). Since the X-ray structure of BOPC is yet to be determined, we constructed its 3-D structure by the homology modeling method. We also constructed an A55T bovine trypsin (A55T BOTR) model for comparison, and investigated the effect of the A55T substitution on the catalytic site structure. The catalytic site of the models was evaluated using molecular dynamics (MD) simulations. Our results show that Val55 causes no serious rearrangement of the catalytic site structure, while the A55T substitution alters His57 into an inactive conformation by the formation of an unusual hydrogen bond between Thr55 Oγ1 and His57 Nε2.

Experimental

Molecular Modeling The models in the present paper were constructed by the CHIMERA modeling system, a program which constructs 3-D protein structures by homology using more than one reference protein. The detailed procedure of CHIMERA is described in our previous paper.[20] The following X-ray structures were taken from the Brookhaven Protein Data Bank[21] (PDB) as reference structures: BOTR (PDB code 4PTP), bovine chymotrypsin (5CHA), human neutrophil elastase (1HNE), the serine protease domain of human u-PA (1LMW), the serine protease domain of human α-thrombin (1PPB), the serine protease domain of human blood coagulation factor Xa (1HCG), rat tonin (1TON), porcine kallikrein (2PKA), porcine elastase (3EST), rat mast cell protease (3RP2) and trypsin from *Streptomyces griseus* (1SGT).

Prior to the BOPC and A55T BOTR models, in order to evaluate the accuracy of the model derived from CHIMERA, we constructed a BOTR model, whose X-ray structure had been solved, using the X-ray structures of other serine proteases as reference structures. The BOTR model was refined by energy minimization with an AMBER united-atom force field[22] using the program APRICOT.[23]

The 3-D structure of BOPC was constructed using CHIMERA. In addition to the above-mentioned X-ray structures, a model structure of the serine protease domain of human protein C (HUPC), which had been built in our laboratory,[24] was used as the reference structure. Because HUPC showed by far the highest sequence identity to BOPC (77%) among the reference proteins, the HUPC model was selected as the base structure for the BOPC model. There was one four-residue deletion in the loop between 1′ and 2′ β-strands in the C-terminal domain (loop 1′–2′) of BOPC in comparison with the sequence of HUPC (Fig. 2). Therefore, the loop 1′–2′ structure (residues 141—155) was taken from the X-ray structure of BOTR (4PTP) because the number of residues in BOTR was equal to BOPC. After the main chain was constructed, the side chains were substituted to obtain the correct amino acid sequence of BOPC. The final structure derived from CHIMERA was refined by energy minimization using APRICOT. The program PROCHECK[25] was used to evaluate the stereochemical quality of the model.

The A55T BOTR model was constructed based on the X-ray structure of BOTR (4PTP) by replacing Ala55 with Thr; it was energy minimized using APRICOT.

Molecular Dynamics Simulation in the Catalytic Region A cap of TIP3P water molecules[26] was placed 22 Å from His57 Cε1 of the models. First, the water molecules were energy minimized, then the whole system was energy minimized. All residues which lie 15 Å or more from His57 Cε1 were fixed, while the residues within 15 Å and the water molecules were allowed to move during the course of MD simulation. The residues that construct the active site were all allowed to move. The whole system was heated from 0 to 300 K for 10 ps, then a 190 ps simulation was performed. The system was kept at 300 K during the productive simulation by applying a temperature coupling τ=0.1 ps. All calculations were carried out using APRICOT with an AMBER united-atom force field, a non-bonded cutoff of 12Å, and a constant dielectric of 1. The SHAKE algorithm[27] was applied to all bonds involving hydrogen atoms. A time step of 0.002 ps was used. Data were collected every 0.5 ps.

```
      16          26          36          46
BOPC  IVDGQEAGWGESPWQAVLLDSKKKLVCGAVLIHVSWVLTV
HUPC  LIDGKMTRRGDSPWQVVLLDSKKKLACGAVLIHPSWVLTA
BOTR  IVGGYTCGANTVPYQVSLNS--GYHFCGGSLINSQWVVSA
                                              *
      56          66          76          86
BOPC  AHCLDSRKKLIVRLGEYDMRRWESWEVDLDIKEVIIHPNY
HUPC  AHCMDESKKLLVRLGEYDLRRWEKWELDLDIKEVFVHPNY
BOTR  AHCY--KSGIQVRLGEDNINVVEGNEQFISASKSIVHPSY
       *
      96          106         116         126
BOPC  TKSTSDNDIALLRLAKPATLSQTIVPICLPDSGLSERKLT
HUPC  SKSTTDNDIALLHLAQPATLSQTIVPICLPDSGLAERELN
BOTR  NSNTLNNDIMLIKLKSAASLNSRVASISLPT------SCA
            *
           136         146         156         166
BOPC  QVGQETVVTGWGYRDE----TKRNRTFVLSFIKVPVVPYN
HUPC  QAGQETLVTGWGYHSSREKEAKRNRTFVLNFIKIPVVPHN
BOTR  SAGTQCLISGWGNTKS----SGTSYPDVLKCLKAPILSDS

                176         186         196
BOPC  ACVHAMENKISENMLCAGILGDPRDACEGDSGGPMVTFFR
HUPC  ECSEVMSNMVSENMLCAGILGDRQDACEGDSGGPMVASFH
BOTR  SCKSAYPGQITSNMFCAGYLEGGKDSCQGDSGGPVVCSGK
                                          *
      206         216         226         236
BOPC  GTWFLVGLVSWGEGCGRLYNYGVYTKVSRYLDWIYGHIKA
HUPC  GTWFLVGLVSWGEGCGLLHNYGVYTKVSRYLDWIHGHIRD
BOTR  ----LQGIVSWGSGCAQKNKPGVYTKVCNYVSWIKQTIAS

      246
BOPC  QEAPLES
HUPC  KEAPQKS
BOTR  N------
```

Fig. 2. Sequence Alignment of BOPC, HUPC and BOTR

Chymotrypsinogen numbering is indicated above the sequences. Residues marked with asterisks are the catalytic triad and Ala/Val55. Portions of the reference proteins used to construct the BOPC model are indicated by bold letters.

Results and Discussion

Construction of the BOTR and BOPC Models We compared the BOTR model constructed by CHIMERA with the corresponding X-ray structure (PDB code 4PTP). The root mean square deviations for superposition between the main chain atoms in the model and those in the X-ray structure are 0.90 Å (all residues) and 0.50 Å (residues lying within 15 Å of His57 Cε1). The BOTR model was very similar to the X-ray structure, especially in the catalytic site region.

The BOPC model was constructed by CHIMERA according to the sequence alignment shown in Fig. 2. To investigate the preferred side chain conformation of Val55, we constructed three structures in which the values of the side-chain χ1 torsional angles of Val55 (N–Cα–Cβ–Cγ1) were 60° (gauche$^-$ conformation, g^-), 180° (trans conformation, t) and −60° (gauche$^+$ conformation, g^+), respectively. Three initial models were refined by energy minimization. The overall structures of the three models are quite similar to one another. The models have two domains containing a six-stranded antiparallel β-sheet each, similar to the reference serine proteases. The models have three disulfide bridges (Cys42–Cys58, Cys168–Cys182 and Cys191–Cys220), which agrees with the experimental data. In the BOPC models, no unfavorable contacts between the atoms and no unnatural chiral centers are observed. The Ramachandran plot of the main-chain torsional angles ϕ–φ of the BOPC models generated by PROCHECK show that all but one of the nonglycine residues are in the most favored or allowed regions (Fig. 3). The exception is Lys138, which is very close to the allowed region. The ω angles are all trans-planar. In all three models,

the hydrogen bonding pattern in the catalytic site is similar to that in Ala55 serine proteases, and the catalytic triad is in the active conformation (Fig. 4). Val55 appears to have no bad effect on the catalytic site.

Evaluation of the BOTR and BOPC Models by Molecular Dynamics Simulations We performed MD simulations of three BOPC models to investigate whether the hydrogen bonding pattern in the catalytic site and the active conformation of the catalytic residues are maintained. In addition to the BOPC models, we performed an MD simulation of the BOTR model to evaluate the dynamic properties of the catalytic site of the model derived from CHIMERA.

The dynamic properties of the hydrogen bonds in the catalytic site are presented in Table 1. In the simulation of the BOTR model, the orientation of the His57 side chain was stably maintained. There was a 180° rotation of the side-chain torsional angle $\chi 2$ of Asp102 (Cα–Cβ–Cγ–Oδ1). This rotation did not distort the hydrogen bonding pattern in the catalytic site, because two conformations of the side chain of Asp102 derived from this rotation were structurally equivalent, and Asp102 Oδ1 and Oδ2 alternated in accepting the hydrogen bonds from Ala56 N, His57 N and Ser214 Oγ. All but two of the hydrogen bonds in the catalytic site were stably maintained during the simulation. The exceptions were the hydrogen bond between His57 Nε2 and Ser195 Oγ, and the hydrogen bond between Asp102 Oδ1/Oδ2 and Ser214 Oγ. The former was lost; this hydrogen bond is thought to be formed after the substrate is bound.[28] The latter was effective 11.5% (between Asp102 Oδ1 and Ser214 Oγ) and 54.5% (between Asp102 Oδ2 and Ser214 Oγ) of the simulation time. This hydrogen bond may not always be necessary for catalysis, because S214A rat anionic trypsin is more active than native ones.[29] The result of the simulation of the BOTR model presented in Table 1 was in good agreement with those of whole unconstrained MD simulations of the X-ray structures of BOTR[30] and porcine pancreatic elastase,[31] suggesting that the catalytic sites of Ala55 serine proteases have similar dynamic properties and that the catalytic region of the model derived from CHIMERA is sufficiently accurate.

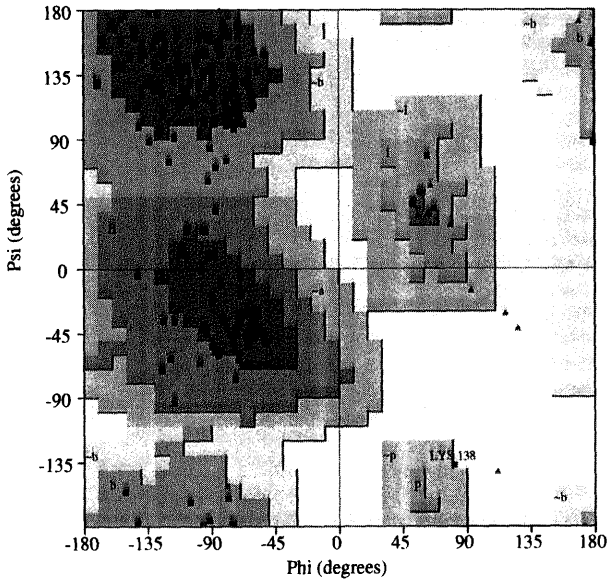

Fig. 3. Ramachandran Plot of the Main Chain Torsional Angles ϕ–φ of the BOPC Model

The ϕ–φ space is divided into four regions: most favored (A, B, L), additional allowed (a, b, l, p), generously allowed (~a, ~b, ~l, ~p), and disallowed. Glycines are represented by triangles. The plot was generated using the program PROCHECK.

For BOPC, independent of the starting conformation, the side chain of Val55 was only in the g^+ conformation during the entire simulation (mean $\chi 1$ values were $-64.5°$ (starting value was 60°), $-65.6°$ (180°) and $-66.0°$ ($-60°$)). The backbone-dependent rotamer library[32] shows that the g^+ conformation is suitable for the backbone conformation of position 55 in this model (mean values of ϕ and φ (ϕ, φ) were ($-97.2°$, 149.0°), ($-98.1°$, 159.6°) and ($-90.8°$, 156.4°)). Table 1 shows that the dynamic properties of the catalytic site of the three simulations were similar to one another. It also indicates that most of the dynamic properties of the catalytic site of BOPC were similar to those of Ala55 serine protease. Only a few hydrogen bonds became a little unstable. For example, though the hydrogen bond between Gly197 O and Val213 N was effective 97.7% of the time for BOTR, it was effective 34.0%, 55.7% and 34.2% of the simulation time for BOPC, which may be due to the slight steric hindrance between Val55 and the neighboring residues. These hydrogen bonds, however, do not adversely affect the active conformations of the catalytic residues. Accordingly, the catalytic residues are maintained normally in BOPC.

A55T BOTR Model In order to investigate the cause of the reduced activity of A55T plasmin, the X-ray structure of

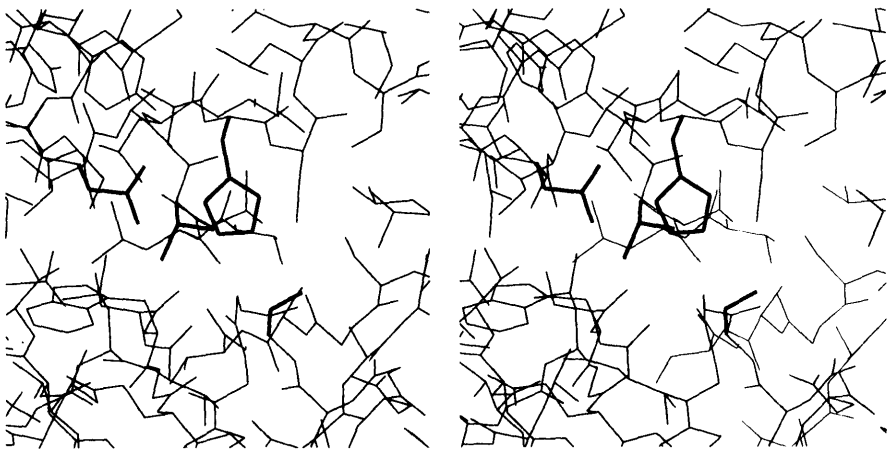

Fig. 4. Stereoview of the Catalytic Site of the BOPC Model

The side chains of the catalytic triad and Val55 are drawn with thicker lines. Val55 is in the g^+ conformation.

Table 1. Hydrogen Bonds in the Catalytic Sites[a] of BOTR and BOPC

Hydrogen bond partners	BOTR model		BOPC model					
	Distance (Å)[b]	Time (%)[c]	Distance (Å)			Time (%)		
			60°[d]	180°	−60°	60°	180°	−60°
A56 N–D102 Oδ1[e]	2.88	79.7	2.87	2.83	2.82	41.7	90.7	98.0
H57 N–D102 Oδ1[e]	2.80	84.2	2.90	2.89	2.90	65.5	98.2	97.2
A56 N–D102 Oδ2[e]	2.91	15.0	2.80	—	—	54.7	0	0
H57 N–D102 Oδ2[e]	2.82	15.5	2.97	—	3.38	35.0	0	0.2
H57 Nδ1–D102 Oδ1[e]	3.01	89.2	2.93	3.09	3.04	82.7	63.7	72.7
H57 Nδ1–D102 Oδ2[e]	2.84	98.5	2.89	2.85	2.86	87.5	98.7	98.7
D102 Oδ1[e]–S214 Oγ	2.91	11.5	—	—	—	0	0	0
D102 Oδ2[e]–S214 Oγ	2.91	54.5	2.80	2.84	2.88	8.2	63.2	36.2
H57 Nε2–S195 Oγ	2.90	0.2	3.09	3.00	3.23	8.2	5.2	10.2
54[f] N–104[f] O	2.97	97.0	2.87	2.87	2.88	99.2	99.5	100
54[f] O–104[f] N	2.86	99.5	2.93	2.91	2.87	94.5	98.7	99.7
G43 O–54[f] Oγ/Oγ1	2.87	93.2	2.91	2.96	2.95	87.0	58.5	91.2
G43 N–S195 O	2.92	96.5	2.97	2.98	2.94	85.7	91.2	93.2
G196 N–V213 O	2.89	99.0	2.92	2.87	2.91	86.0	97.5	91.5
G197 O–V213 N	2.94	97.7	3.15	3.09	3.18	34.0	55.7	34.2

a) The hydrogen bonds in the catalytic site are schematically shown in Fig. 1. *b*) The distances are average distances of snapshots where the interactions are characterized as hydrogen bonds (2.4—3.4 Å) during MD simulations. *c*) Times (%) are percentages of snapshots where the interactions are characterized as hydrogen bonds during MD simulations. *d*) The starting $\chi 1$ values of Val55 in MD simulations of BOPC. *e*) When there are rotations of the $\chi 2$ angle of Asp102, Asp102 Oδ1 and Oδ2 alternate in accepting the hydrogen bonds from Ala56 N, His57 N, His57 Nδ1 and Ser214 Oγ. *f*) Positions 54 and 104 are Ser and Met in BOTR, and Thr and Ala in BOPC, respectively.

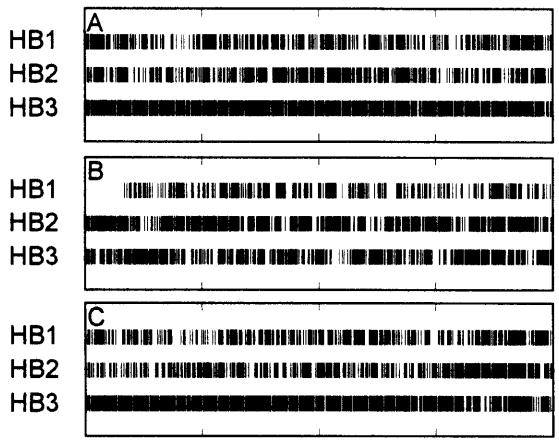

Fig. 5. Dynamic Properties of the Hydrogen Bonds of A55T BOTR in MD Simulations

Small bars denote the formation of the hydrogen bonds between Thr55 Oγ1 and His57 Nε2 (HB1), between His57 Nδ1 and Asp102 Oδ1 (HB2) and between His57 Nδ1 and Asp102 Oδ2 (HB3). The starting $\chi 1$ values of Thr55 were 60° (A), 180° (B) and −60° (C).

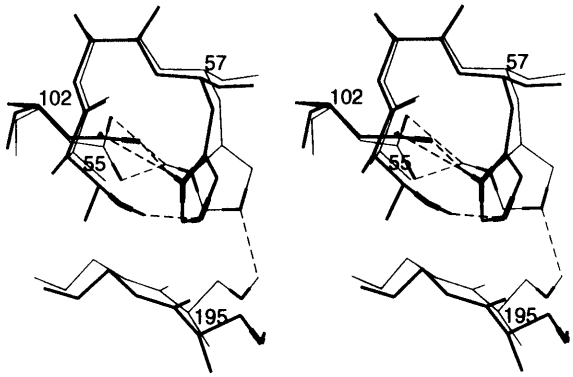

Fig. 6. Stereoview of the Catalytic Triad and Ala/Thr55 in Normal BOTR (Thin Line) and A55T BOTR (Thick Line)

Thr55 Oγ1, His57 Nδ1, His57 Nε2, Asp102 Oδ atoms and Ser195 Oγ are stressed with bold lines in each structure. The hydrogen bonds are drawn with dotted lines. The hydrogen atoms (Thr55 HOγ1, His57 HNδ1 and Ser195 HOδ) are shown.

plasmin would be useful, but has not been solved. Therefore, we constructed an A55T BOTR model based on the X-ray structure of BOTR to investigate the effect of replacing Ala55 with Thr upon the structure of the catalytic site. We constructed three models, in which the $\chi 1$ values of Thr55 (N–Cα–Cβ–Oγ1) were 60° (g^-), 180° (t) and −60° (g^+), and evaluated them using MD simulations. Independent of the starting conformation, Thr55 was only in the g^- conformation (mean $\chi 1$ values were 34.3° (starting value was 60°), 30.0° (180°) and 32.8° (−60°)), which is equivalent to the g^+ conformation of Val55 in BOPC because of the definition of the $\chi 1$ angles. The backbone-dependent rotamer library[32] shows that the preferred side chain conformation of Thr is strongly dependent on the backbone conformation, and the g^- conformation is most suitable for the backbone conformation of position 55 in this model (mean values of ϕ and φ (ϕ, φ) are (−71.2°, 155.3°), (−71.9°, 150.3°) and (−71.7°, 153.5°)). The most remarkable feature of A55T BOTR is an unusual conformation of the His57 side chain due to the A55T substitution (Figs. 5, 6). Thr55 Oγ1 and His57 Nε2 electrostatically interact with one another through Thr55 HOγ1, forming a new hydrogen bond, though this hydrogen bond is out of the His57 imidazole plane at mean angles of 88.4°, 84.7° and 88.2°. It is never formed in Ala55 serine proteases and BOPC, because the side chain of Ala/Val55 includes no hetero atoms that can be a hydrogen bond donor to His57 Nε2. The normal hydrogen bonds between His57 Nδ1 and Asp102 Oδ atoms were also maintained stably, and, therefore, His57 Nδ1 and Nε2 were hydrogen bonded to both Asp102 Oδ atoms and Thr55 Oγ1, respectively. His57 Nε2 retreats from Ser195 Oγ to accept the hydrogen bond from Thr55 Oγ1. Table 2 shows that the dynamic properties of the hydrogen bonds in the catalytic site of three MD simulations were similar to one another. Although the hydrogen bond between Gly43 O and Ser54 Oγ was effective 93.2% of the simulation time for BOTR (Table 1), it was effective 66.2%, 68.5% and 52.7% of the time for A55T BOTR. This

Table 2. Hydrogen Bonds in the Catalytic Site[a] of A55T BOTR

Hydrogen bond partners	A55T BOTR model					
	Distance (Å)[b]			Time (%)[c]		
	60°[d]	180°	−60°	60°	180°	−60°
A56 N–D102 Oδ1[e]	2.74	2.82	2.78	96.5	33.2	80.5
H57 N–D102 Oδ1[e]	2.93	2.97	2.90	96.2	41.5	81.7
A56 N–D102 Oδ2[e]	2.89	2.75	2.70	2.2	65.5	18.0
H57 N–D102 Oδ2[e]	3.33	2.94	2.88	1.2	63.7	17.2
H57 Nδ1–D102 Oδ1[e]	3.08	2.88	3.02	74.7	82.7	72.7
H57 Nδ1–D102 Oδ2[e]	2.77	2.97	2.80	99.2	78.2	96.0
D102 Oδ1[e]–S214 Oγ	—	2.88	2.92	0	3.5	0.2
D102 Oδ2[e]–S214 Oγ	2.85	2.77	2.83	35.7	15.0	28.7
H57 Nε2–S195 Oγ	3.26	3.19	3.12	0.7	0.7	2.2
S54 N–M104 O	2.94	2.93	2.95	98.0	97.5	98.5
S54 O–M104 N	2.87	2.84	2.85	99.5	100	100
G43 O–S54 Oγ	2.97	2.97	2.97	66.2	68.5	52.7
G43 N–S195 O	2.95	2.97	3.00	94.0	92.0	83.2
G196 N–V213 O	2.93	2.91	2.91	98.2	99.0	98.7
G197 O–V213 N	2.96	2.93	2.99	97.5	98.7	97.2

Definitions of *a*)—*c*) and *e*) are the same as those in Table 1. *d*) The starting χ1 values of Thr55 in MD simulations.

Table 3. Hydrogen Bonds in the Catalytic Site[a] of BOPC-X

Hydrogen bond partners	BOPC-X model	
	Distance (Å)[b] −60°[d]	Time (%)[c] −60°
A56 N–D102 Oδ1[e]	2.72	39.2
H57 N–D102 Oδ1[e]	2.97	34.5
A56 N–D102 Oδ2[e]	2.78	59.0
H57 N–D102 Oδ2[e]	2.96	53.0
H57 Nδ1–D102 Oδ1[e]	2.89	76.2
H57 Nδ1–D102 Oδ2[e]	2.92	79.2
D102 Oδ1[e]–S214 Oγ	2.90	14.7
D102 Oδ2[e]–S214 Oγ	2.75	4.2
H57 Nε2–S195 Oγ	3.16	3.0
T54 N–A104 O	2.98	97.5
T54 O–A104 N	2.85	100
G43 O–T54 Oγ1	2.91	96.0
G43 N–S195 O	2.90	98.0
G196 N–V213 O	2.93	98.7
G197 O–V213 N	2.96	95.5

Definitions of *a*)—*c*) and *e*) are the same as those in Table 1. *d*) The starting χ1 value of Val55 in MD simulation.

is probably due to the hindrance caused by the A55T substitution.

Effect of Val55 and Thr55 on the Catalytic Site As described above, the BOPC model shows that Val55 causes no serious rearrangement of the catalytic site structure, while in the case of A55T BOTR, the unusual hydrogen bond between Thr55 Oγ1 and His57 Nε2 due to the A55T substitution alters His57 into the unusual conformation. In the catalytic mechanism of normal serine proteases, the formation of the strong hydrogen bond between Ser195 Oγ and His57 Nε2 is essential after the substrate binds, which enables His57 Nε2 to accept a proton from Ser195 Oγ as the catalytic base (drawn with a thin line in Fig. 6). In the case of A55T BOTR, however, it is difficult for His57 to accept a proton from Ser195, because His57 Nε2 stably accepts a hydrogen bond from Thr55 Oγ1 and retreats from Ser195 Oγ (drawn with a thick line in Fig. 6). This indicates that His57 in A55T BOTR is unable to act as the catalytic base and to enhance the nucleophilicity of Ser195. The studies of D102N rat trypsin demonstrate that the inability of His57 to act as the catalytic base reduces protease activity.[1,2] Though the A55T plasmin model itself was not constructed, the cause of reduced activity of A55T plasmin is probably the inability of His57 to act as the catalytic base.

The X-ray structures of serine proteases, which are all Ala55 serine proteases, show that the region where the proton transfer from Ser195 to His57 occurs is completely conserved in both the primary and tertiary structures throughout this family. Moreover, this region is stabilized by the hydrogen bonding network conserved in this family. In this region, there are no hetero atom candidates for the hydrogen bond donor to His57 Nε2 except Ser195 Oγ, which probably ensures the proton transfer from Ser195 Oγ to His57 Nε2 after the substrate binds. In the case of BOPC, it is probable that Val55 causes no serious rearrangement of the catalytic site structure because the Val side chain has no hetero atoms to cause disorder within the active conformation of the catalytic residues. This indicates that BOPC which includes Val55 works nearly as effectively as Ala55 serine proteases. In almost all serine proteases, however, position 55 is Ala instead of Val. Though the cause of the high conservation of Ala55 is unknown at present, the exceptional Val55 shows that the side chain at position 55 is not necessarily Ala because of the fact that the essential side chains for catalysis, such as the catalytic triad, are completely conserved without exception. The side chains that do not inhibit the active conformation of the catalytic residues are suitable for position 55. We also constructed a model of plaice trypsin with Val55. Its catalytic site was very similar to that of BOPC, and thus it may be active for the same reason as BOPC.

Conclusion

In conclusion, the present study demonstrates that the residue at position 55 provides an important contribution to the active conformation of the catalytic residues. In the case of the A55T variant, since His57 Nε2 strongly accepts the unusual hydrogen bond from Thr55 Oγ1 and retreats from Ser195 Oγ, His57 is unable to accept the serine hydroxyl proton and to enhance the nucleophilicity of Ser195. The reduced activity of A55T plasmin is probably caused by the inability of His57 to act as the catalytic base. On the other hand, in the case of Ala55 serine proteases and BOPC, Ala/Val55 has no hetero atoms that can be a hydrogen bond donor to His57 Nε2, and, therefore, His57 is in the active conformation and is able to accept a proton from Ser195 as the catalytic base after the substrate is bound. The present study will shed new light on the essential environment for the catalysis of serine proteases.

Note In this article, the HUPC model was used as the reference structure when we constructed the BOPC model. Recently, the X-ray structure of HUPC has been deposited with PDB (PDB code 1AUC). Therefore, we constructed another BOPC model (BOPC-X model) following the same method using the X-ray structure of HUPC instead of the HUPC model as the reference structure for comparison. The root mean square deviations for superposition between the main chain atoms in the former BOPC and latter BOPC-X models are 1.10 Å (all residues) and 0.54 Å (residues lying

within 15 Å of His57 Cε1). Both models were quite similar to each other, especially in the catalytic site region. We evaluated the catalytic site of the BOPC-X model using MD simulation. The starting conformation of Val55 was g^+, because the former BOPC model and the backbone-dependent rotamer library[32] showed that the preferred conformation for Val55 was g^+. As a result, the active conformation of the catalytic site is maintained normally with the g^+ conformation of Val55 (mean $\chi 1$ value was $-67.5°$) in the latter BOPC-X model like in the former BOPC model (Table 3). That Val55 has no bad effect on the catalytic site is shown by the both BOPC and BOPC-X models.

Acknowledgments We thank Dr. Shigetaka Yoneda for helpful discussion. This work was supported by a grant-in-aid for special project research from the Ministry of Education, Science, Sports and Culture in Japan.

References

1) Sprang S., Standing T., Fletterick R. J., Stroud R. M., Finer-Moore J., Xuong N. H., Hamlin R., Rutter W. J., Craik C. S., *Science*, **237**, 905—909 (1987).
2) Craik C. S., Roczniak S., Largman C., Rutter W. J., *Science*, **237**, 909—913 (1987).
3) Corey D. R., Craik C. S., *J. Am. Chem. Soc.*, **114**, 1784—1790 (1992).
4) Corey D. R., McGrath M. E., Vásquez J. R., Fletterick R. J., Craik C. S., *J. Am. Chem. Soc.*, **114**, 4905—4907 (1992).
5) Umeyama H., Hirono S., Nakagawa S., *Proc. Natl. Acad. Sci. U.S.A.*, **81**, 6266—6270 (1984).
6) Warshel A., Naray-Szabo G., Sussman F., Hwang J. K., *Biochemistry*, **28**, 3629—3637 (1989).
7) Rypniewski W. R., Perrakis A., Vorgias C. E., Wilson K. S., *Protein Eng.*, **7**, 57—64 (1994).
8) Lesk A. M., Fordham W. D., *J. Mol. Biol.*, **258**, 501—537 (1996).
9) Stenflo J., Fernlund P., *J. Biol. Chem.*, **257**, 12180—12190 (1982).
10) Leaver M. J., George S. G., *EMBL*, AC X56744, (1992).
11) Rypniewski W. R., Perrakis A., Vorgias C. E., Wilson K. S., *Protein Eng.*, **7**, 57—64 (1994).
12) Miyata T., Iwanaga S., Sakata Y., Aoki N., *Proc. Natl. Acad. Sci. U.S.A.*, **79**, 6132—6136 (1982).
13) Miyata T., Iwanaga S., Sakata Y., Aoki N., Takamatsu J., Kamiya T., *J. Biochem.* (Tokyo), **96**, 277—287 (1984).
14) Ichinose A., Espling E. S., Takamatsu J., Saito H., Shinmyozu K., Maruyama I., Petersen T. E., Davie E. W., *Proc. Natl. Acad. Sci. U.S.A.*, **88**, 115—119 (1991).
15) Li L., Kikuchi S., Arinami T., Kobayashi K., Tsuchiya S., Hamaguchi H., *Clin. Genet.*, **45**, 285—287 (1994).
16) Tsutsumi S., Saito T., Sakata T., Miyata T., Ichinose A., *Thromb. Haemostasis*, **76**, 135—138 (1996).
17) Murata M., Ooe A., Izumi T., Nakagawa M., Takahashi S., Ishikawa M., Mori K., Ichinose A., *Brit. J. Haemoto.*, **99**, 301—303 (1997).
18) Aoki N., Moroi M., Sakata Y., Yoshida N., *J. Clin. Invest.*, **61**, 1186—1195 (1978).
19) Sakata Y., Aoki N., *J. Biol. Chem.*, **255**, 5442—5447 (1980).
20) Yoneda T., Komooka H., Umeyama H., *J. Protein. Chem.*, **16**, 597—605 (1997).
21) Bernstein F. C., Koetzle T. F., Williams G. J. B., Meyer E. F., Jr., Brice M. D., Rodgers J. R., Kennard O., Shimanouchi T., Tasumi M., *J. Mol. Biol.*, **112**, 535—542 (1977).
22) Weiner S. J., Kollman P. A., Case D. A., Singh U. C., Ghio C., Alagona G., Profeta Jr. S., Weiner P., *J. Am. Chem. Soc.*, **106**, 765—784 (1984).
23) Yoneda S., Umeyama H., *J. Chem. Phys.*, **97**, 6730—6736 (1992).
24) Miyata T., Sakata T., Zheng Y. Z., Tsukamoto H., Umeyama H., Uchiyama S., Ikusaka M., Yoshioka A., Imanaka Y., Fujimura H., Kambayashi J., Kato H., *Thromb. Haemostasis*, **76**, 302—311 (1996).
25) Laskowski R. A., McArthur M. W., Moss D. S., Thornton J. M., *J. Appl. Crystallogr.*, **26**, 283—291 (1993).
26) Jorgensen W. L., Chandrasekhar J., Madura J. D., *J. Chem. Phys.*, **79**, 926—935 (1983).
27) Ryckaert J. P., Ciccotti G., Berendsen H. J. C., *J. Comp. Phys.*, **23**, 327—341 (1977).
28) Perona J. J., Craik C. S., *Protein Sci.*, **4**, 337—360 (1995).
29) McGrath M. E., Vásquez J. R., Craik C. S., Yang A. S., Honig B., Fletterick R. J., *Biochemistry*, **31**, 3059—3064 (1992).
30) Heimstad E. S., Hansen L. K., Smalås A. O., *Protein Eng.*, **8**, 379—388 (1995).
31) Geller M., Carlson-Golab G., Lesyng B., Swanson S. M., Meyer E. F., Jr., *Biopolymers*, **30**, 781—796 (1990).
32) Dunbrack R. L., Jr., Karplus M., *J. Mol. Biol.*, **230**, 543—574 (1993).